

## ***An Arrangement of Flow Velocities and Turbulence Profiles of Co-Axial Cold Jet***

Yuzuru SHIMAMOTO \* and Yutaka TANAKA \*

(Received December 20, 1975)

### Synopsis

Results of calculations and experiments on the cold co-axial flow presented in this paper are summarized as follows ;

(1) A theoretical expression method for co-axial flow field of two dimension is investigated to estimate more exactly the flow profile and the velocity gradient.

(2) Measurements of mixing length were carried out for the confined co-axial jet flow. On the basis of measured data, inquiry is made for the propriety of the assumption proposed in the previous paper (1) that the mixing length may be expressed as a function of the minimum distance to the nearby wall.

(3) Experimental inquiry was also done on the co-relation between Lagrangian length scale and the mixing length.

### 1. Introduction.

For the last forty years, new theories of turbulence which are full of variety in content, form and applicability have been found in literature; most of them are successful in explaining turbulence phenomena. However, recently the analytical treatment of turbulence properties such as velocity and concentration fluctuations are being re-examined on the purpose of application to the simulation of turbulent diffusion flame. The purpose of these re-examination is to derive the more skillful turbulence model on the standpoints of applicability, accuracy, economy of computer time and simplicity.

The mathematical models of turbulence are classified into three large groups, that is, algebraic turbulence-viscosity models, differential turbulence-viscosity models and models employing differential expressions for stresses of turbulences. The first two groups employ Boussinesq's or Prandtl's suggestion that the stress-strain relation for turbulent flows could be represented in the same form as that for a Newtonian fluid in laminar motion. The third group of model includes those that dispense with the notion of effective turbulence properties and, instead, provide

---

\* Department of Mechanical Engineering

differential transport equations for the turbulent fluxes themselves. It is difficult to prefer the best one from the above models, because the availability of models vary with subjects of study. In order to solve the set of differential equations governing the flow fields, even if the best model is used for analysis, some global assumptions must be given for the factors, such as mixing length, turbulence length scale, turbulence strength and non-homogeneity.

In our last two papers on the simulation method of diffusion flames with co-axial swirl flow (1,2), the algebraic model in which the time-mean deformation tensor is connected with the viscosity are used from the standpoints of both the reduction of computation time and the simplicity. In this model the mixing length are assumed as a function of the minimum distance to solid walls. The first purpose of this report is to examine the propriety of this assumption through the measurement of the mixing length variations in the regions where the flow fields vary remarkably. Since the turbulence measurement is not easy for a co-axial flow with swirl and combustion, the experiment has been carried out for iso-thermal co-axial flows without swirl.

The second purpose is to express the steady field obtained for confined flow as functions of axial and radial distances. This expression is necessary to treat theoretically the profile of the flow, in which the deformation tensors can not be simply expressed as a radial gradient of axial velocity.

The third purpose is to study whether Lagrangian scale of turbulence may be estimated from the mixing length or not. Although both moment of turbulence and time-mean velocity profile must be measured to obtain the mixing length, only the moment is required for the determination of the Lagrangian scale of turbulence. If this estimation is applicable, the troublesome task for measuring the mixing length may be largely reduced. However the measured data revealed that the distribution tendency of Lagrangian scale is different from that of mixing length.

## 2. Nomenclature.

$a_j, c_{i,j}$	coefficients of Fourier transforms	$\rho$	density
$L$	flow distance required to reach ultimate velocity profile (entrance length)	$\tau$	stress
$l$	mixing length or length scale of turbulence	Subscripts	
$R$	pipe radius	1, 2	direction for x and r respectively
$R(\tau)$	coefficients of correlation at the time difference $\tau$	L	for Lagrangian scale of turbulence
$t, T$	time	p	primary flow
$u, U$	flow velocity	s	secondary flow
$z$	minimum distance to solid wall	Superscripts	
$x$	axial distance from nozzle exit	'	turbulence component
$r$	radial distance from center line of jet	-	time - mean component

## 3. Apparatus and procedures.

The basic structure of test apparatus consists of two co-axial circular pipes. The outer side pipe has inner diameter ( $=2R$ ) of 98 mm, the inner side one has inner diameter of 16 mm and thickness of 3 mm at the outlet. Hereafter, the properties of inner side pipe (nozzle) and annular parts between two pipes are expressed as primary and secondary

ones, respectively.

For the measurement of time - mean velocity, a set of dynamic and static pressure tubes were used. The former outer and inner diameters are 2 mm and 3 mm respectively. The static pressure tube is illustrated in Fig. 1. The pressure difference of these tubes was measured with a X-type hot wire probe, and a set of anemometers and linealizers. The outputs of these instruments are recorded by a data recorder, then the recorded tape is processed by a high speed data analyzer of our School of Engineering.

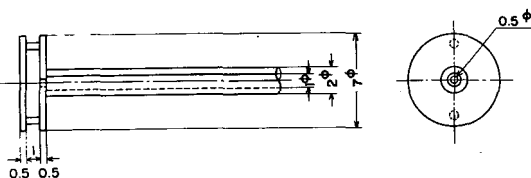


Fig. 1 . Static pressure tube.

#### 4. Procedures for analysis.

##### 4-1. Fully developed velocity profile.

In any case of entrance profile, the flow of co-axial jet in a confined fields are developed, reaching an ultimately developed profile. If the pressure and density changes between the entrance and the fully developed section are negligible, the fully developed velocity profile is supposedly expressed by the following approximation with modified  $1/n$  - th power law,

$$\begin{aligned} 0 \leq r \leq r_0, \quad U_{1,\infty} &= U_{\max} [1 - (r/R)^2], \\ r_0 \leq r \leq R, \quad U_{1,\infty} &= U_{\max} [1 - (r_0/R)^2] [(R-r)/(R-r_0)]^{1/n}. \end{aligned} \quad (1)$$

Denoting the ratio of sectional-mean to maximum velocity by  $Ru$ ,

$$Ru = U_{\text{mean}} / U_{\max} . \quad (2)$$

From Eq.(1),  $Ru$  and radial distance ratio  $r_0/R$  become functions of the index  $n$ ,

$$Ru = \frac{64 n^6 - 128 n^5 + 112 n^4 - 56 n^3 + 18 n^2 - 5 n + 1}{2(n+1)(2n+1)(2n-1)^4}, \quad (3)$$

$$r_0/R = 1 / (2n - 1) . \quad (4)$$

From the data obtained by Nikuradse (3), the index  $n$  is expressed as a function of the Reynolds number  $Re$ .

$$\text{For turbulent region of } Re \geq 5 \times 10^3, \quad n = 4 (Re/10^3)^{0.1386},$$

$$\text{for transition region of } 5 \times 10^3 \geq Re \geq 10^3, \quad n = Re/10^3,$$

$$\text{for laminar region of } 10^3 \geq Re \geq 0, \quad n = 1 . \quad (5)$$

Entrance length  $L$  is expressed usually as follows ;

$$\text{for laminar flow,} \quad L = 0.106 Re R,$$

$$\text{for turbulent flow,} \quad L = 60 R . \quad (6)$$

The Fourier series of order  $n_2$  of Eq.(1) become ,

$$\bar{u}_{1,\infty}(r) = -a_1/2 + \sum_{j=1}^{n_2} a_j \cos[(j-1)\pi r/R], \quad (7)$$

where coefficients  $a_j$  are represented by

$$a_j = (2/R) \int_0^R U_{1,\infty}(r) \cos[(j-1)\pi r/R] dr. \quad (8)$$

#### 4-2. Velocity profile.

Denoting the difference of the measured axial velocity profiles  $U_1(x,r)$  and the fully developed velocity profiles  $U_{1,\infty}(r)$  by a symbol  $F(x,r)$ , then the axial velocity equation of two dimension can be obtained by the double integral procedure of  $F(x,r)$  as follows ;

$$\begin{aligned} \bar{u}_1(x,r) = & -(a_1/2) - c_{1,1}/4 - (1/2) \left\{ \sum_{i=1}^{n_1} c_{i,1} \cos[(i-1)\pi x/L] \right. \\ & + \sum_{j=1}^{n_2} (c_{1,j} - 2a_j) \cos[(j-1)\pi r/R] \left. \right\} + \sum_{j=1}^{n_2} \sum_{i=1}^{n_1} c_{i,j} \\ & \cdot \cos[(j-1)\pi r/R] \cos[(i-1)\pi x/L], \end{aligned}$$

$$\text{where } c_{i,j} = (2/LR) \int_0^L \int_0^R F(x,r) \cos[(j-1)\pi r/R] \cos[(i-1)\pi x/L] dr \cdot dx \quad (9)$$

The homogeneous density approximation gives the next equation of continuity,

$$\frac{\partial \bar{u}_1}{\partial x} + \frac{\partial \bar{u}_2}{\partial r} + \frac{\bar{u}_2}{r} = 0, \quad (10)$$

The boundary conditions of  $\bar{u}_2(x,r)$  are

$$\begin{aligned} \frac{\partial \bar{u}_2}{\partial r} &= 0 \quad \text{at } r = 0, \\ \bar{u}_2 &= 0 \quad \text{at } r = R. \end{aligned} \quad (11)$$

From the Eqs.(9),(10) and (11), the radial flow velocity  $\bar{u}_2(x,r)$  is obtained as ,

$$\begin{aligned} \bar{u}_2(x,r) = & (\pi R/4L) \sum_{i=2}^{n_1} c_{i,1} [(i-1) \sin[(i-1)\pi x/L] + (R^2/L)] \\ & \cdot \sum_{j=2}^{n_2} \sum_{i=2}^{n_1} c_{i,j} [(i-1)/(j-1)^2] \sin[(i-1)\pi x/L] \\ & \cdot \{ [\cos[(j-1)\pi r/R] - 1] / r + [(j-1)\pi/R] \\ & \cdot \sin[(j-1)\pi r/R] \}, \end{aligned} \quad (12)$$

#### 4-3. Turbulence properties.

Turbulence components  $u_1'$  and  $u_2'$  of velocity are obtained from the

sum and the difference of two AC outputs of X-type hot wires respectively. By numerical computation of these measured analogous data, the stresses  $\tau_{11}$ ,  $\tau_{22}$  and  $\tau_{12}$  are obtained as follows;

$$\begin{aligned}\tau_{11} &= -\overline{\rho u_1' u_1'} , \\ \tau_{22} &= -\overline{\rho u_2' u_2'} , \\ \tau_{12} &= -\overline{\rho u_1' u_2'} .\end{aligned}\tag{13}$$

If  $d$  represents the deformation velocity tensor, the square of mixing length from the expansion of Prandtl's hypothesis is expressed as,

$$l^2 = [ \tau_{12} / \rho ] ( \bar{d} : d/2 )^{-1/2} .\tag{14}$$

Since there is no tangential components of velocity, Eq.(14) can be simplified as,

$$l^2 = \tau_{12} / [ \rho ( \frac{\partial \bar{u}_1}{\partial r} + \frac{\partial \bar{u}_2}{\partial x} ) \sqrt{ ( \frac{\partial \bar{u}_1}{\partial r} )^2 + ( \frac{\partial \bar{u}_2}{\partial x} )^2 } ] .\tag{15}$$

The mixing length can be calculated by using  $\bar{u}_1$ ,  $\bar{u}_2$  and  $\tau_{12}$  obtained from Eq.(9), (12) and (13) respectively.

Coefficients of self correlation  $R_1(\tau)$  and  $R_2(\tau)$  are represented by the equation ;

$$R_k(\tau) = \int_0^T u_k'(x,r,t) u_k'(x,r,t+\tau) dt / [ \overline{u_k' u_k'} T ] ,\tag{16}$$

where  $k$  represents directional index for 1 or 2 and  $T$  represents time interval which is long enough with respect to the time of turbulence oscillation. Then the Lagrangian scale of turbulence  $l_{k,L}$  can be estimated by the next numerical integration ,

$$l_{k,L} = \sqrt{\overline{u_k' u_k'}} \int_0^\tau \text{for } R_k(\tau)=0 \quad R_k(\tau) d\tau .\tag{17}$$

## 5. Results and discussions.

### 5-1. Time-mean velocity profile.

There exist two types of flow pattern which are characterized by the ratio of the primary nominal flow velocity  $u_{1p}$  to the secondary nominal flow velocity  $u_{1s}$ . One is a jet type flow and other is a wake type flow.

Figure 2 shows the  $\bar{u}_1$ - profiles for the velocity groups (8,4), (2,4) and (0,4). Two figures in the parentheses mean a group of  $u_{1p}$  and  $u_{1s}$  as  $(u_{1p}, u_{1s})$ . The plotted points in Fig.2 indicate the measured data. The curves obtained by means of Fourier transform coincide with the curve which pass smoothly through these plotted points. It is known from the figures that extreme values in the  $u_1$ -profiles are classified into three kinds. The one is a maximum or a minimum value at the center axis [C.A.L], the second is seen in the secondary flow field [S.F.L], and the third is a extreme minimum value in the mixing region which lies between the primary and the secondary flow fields [M.R.L].

In Figure 3 the extreme values measured and obtained from Fourier

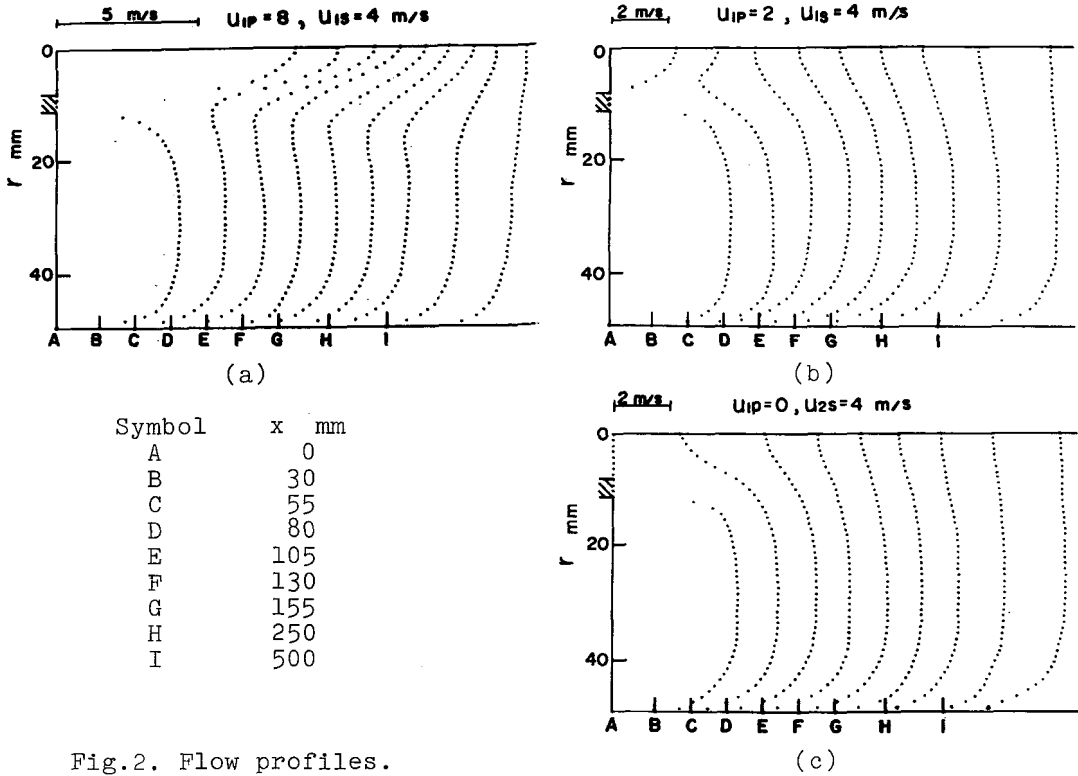


Fig. 2. Flow profiles.

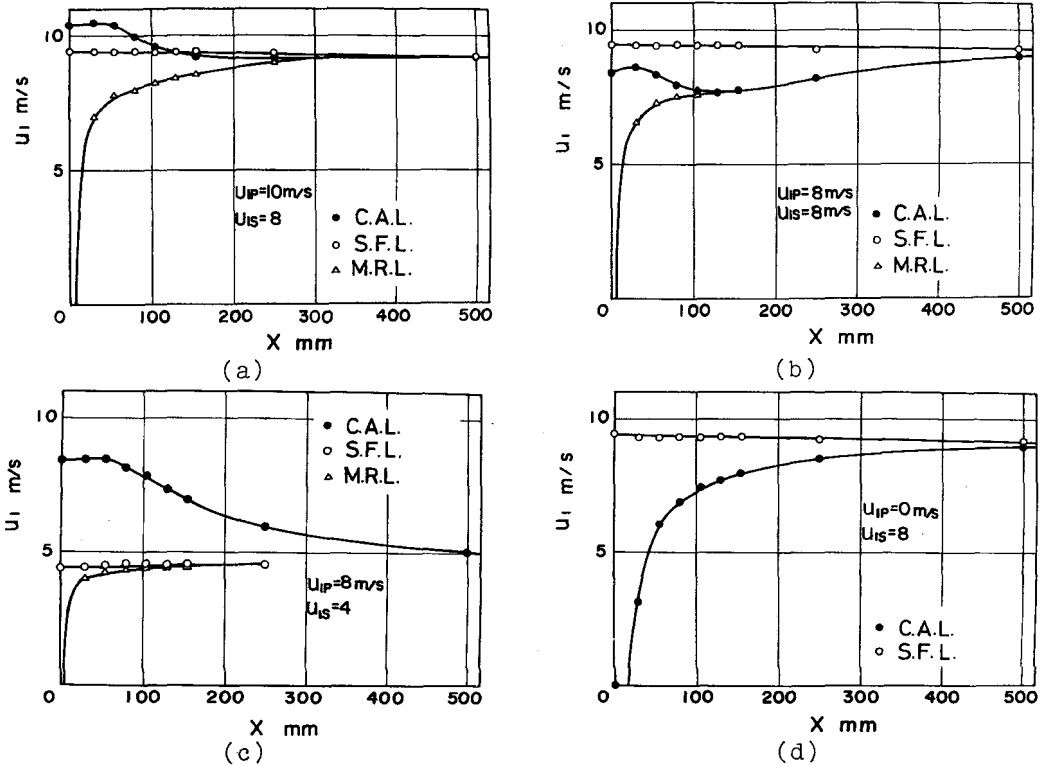
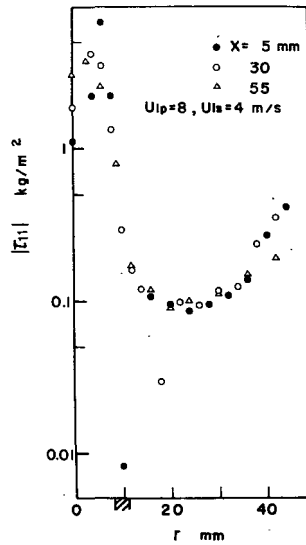


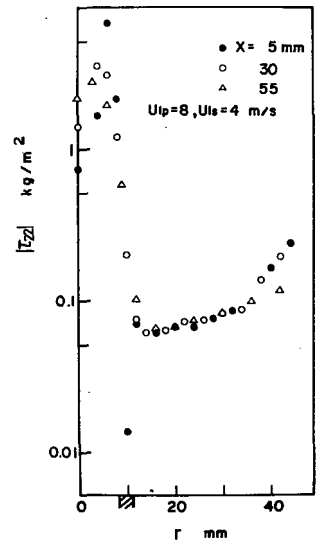
Fig. 3. Longitudinal changes of extreme velocities.

transform curves are shown for the nominal velocity groups of (10,8) , (8,8) , (8,4) and (0,3). For (10,8) and (8,8), it is known that the velocity at centerline (C.A.L) increases initially and then decreases gradually with increase in axial distance. Thereafter it is mixed with M.R.L. and reaches gently to S.F.L. As is illustrated in these figures, there apparently exist some regions where the velocity at C.A.L. becomes smallest in the range of about  $x=100$  mm to 200 mm. The extreme values for (8,4) show more complex feature. S.F.L. is begin to compose with M.R.L. at the nozzle exit, and then they disappear in the regions from  $x = 200$  mm to  $x = 300$  mm. For the case of no primary flow ( 0.8 ), C.A.L. approximately coincide with M.R.L. and the flow profile becomes typical wake type. For

the reason of these complex feature, the velocity profiles in the vicinity of the nozzle exit can not be simply expressed by a half value width of the jet and the difference between C.A.L. and S.F.L. This mentions that the velocity profile with confined secondary flow has features essentially different from the velocity profile without the secondary flow such as free jet. The reasons for the use of two dimensional expression by Fourier transformation stand mainly on these experimental facts.



(a)



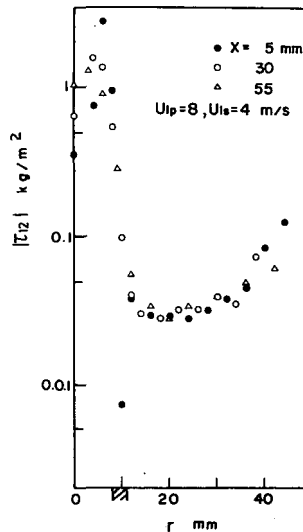
(b)

5-2. Turbulence properties.

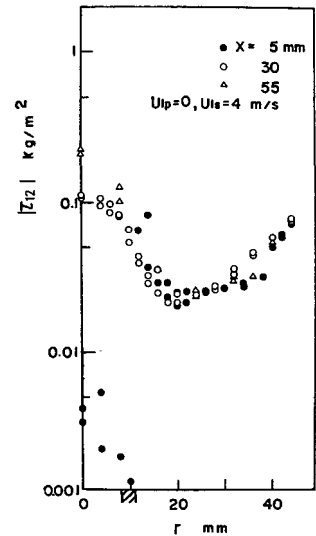
Figure 4-(a), (b), (c) and (d) indicate the turbulence stresses  $\tau_{11}$ ,  $\tau_{22}$  and  $\tau_{12}$  for (8,4) and  $\tau_{12}$  for (0,4) respectively.

These value become maximum at the maximum velocity gradient in the mixing region, as was shown by Tani and Kobashi (4). They take high value in the regions near outer solid wall, however, they exhibit contrast tendency at the nearby regions of primary nozzle port. While, the longitudinal change of  $\tau$  in the secondary field is quite small.

Figure 5 indicates the mixing length which was calculated from the measured data of the shear stress  $\tau_{12}$  and the time



(c)



(d)

Fig.4. Turbulence stresses  $\tau_{11}$ ,  $\tau_{22}$  and  $\tau_{12}$ .

mean velocities  $\bar{u}_1$  and  $\bar{u}_2$ .  $l$  takes large values in the vicinity of center line and in the region of secondary flow field. As was described in the introduction, this tendency shows that the mixing length becomes larger with decrease in the distance from the nearby solid wall. In figure 6, the relation between the minimum distance to the nearby solid wall  $z$  and the mixing length  $l$  are re-illustrated for many groups of  $u_{1p}$

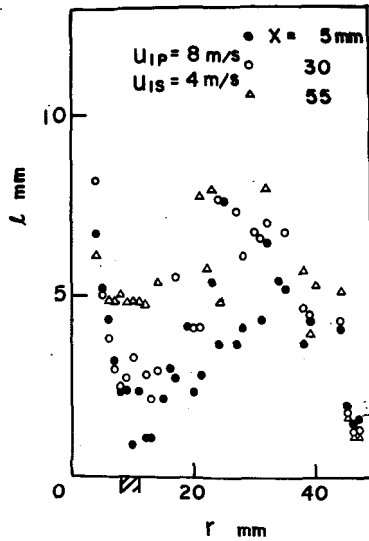


Fig.5. Mixing length as a function of radial distance  $r$ .

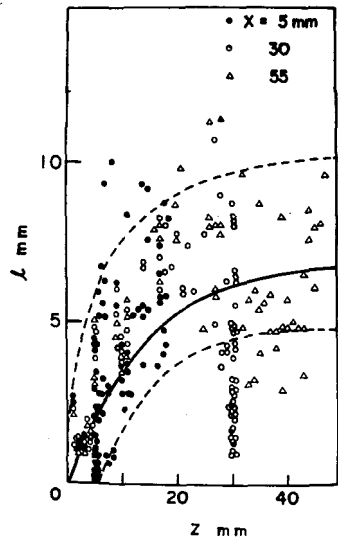
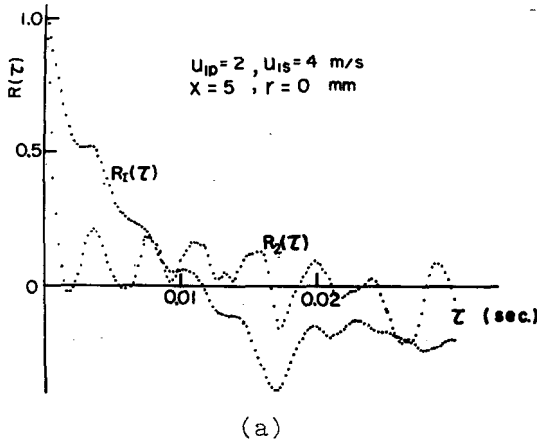
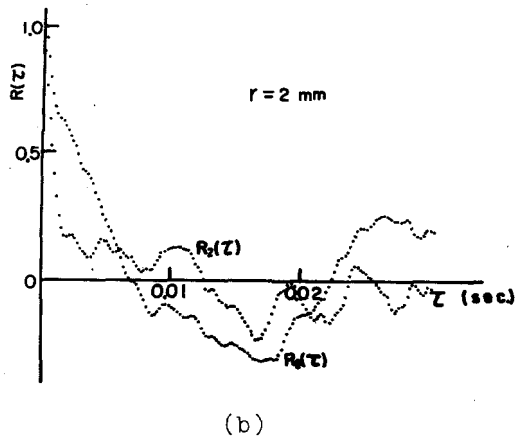


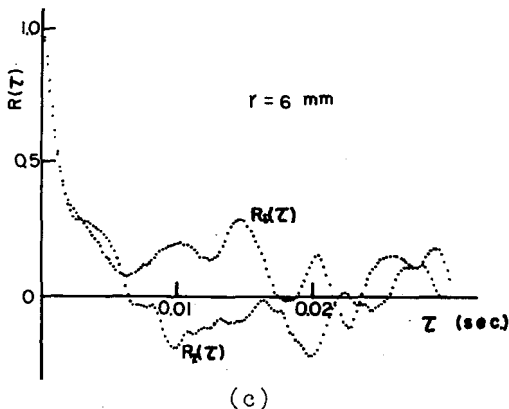
Fig.6. Mixing length as a function of  $z$ .



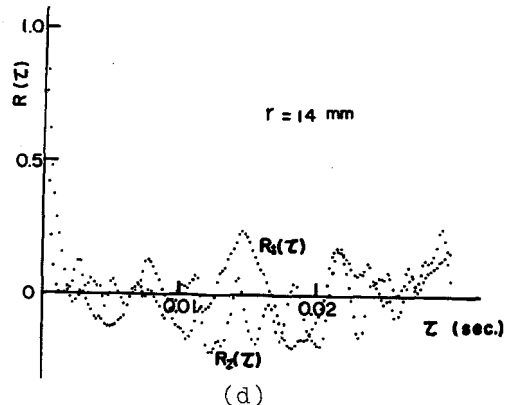
(a)



(b)



(c)



(d)

Fig.7. Coefficients of self correlation  $R_1$  and  $R_2$  for the velocity group of (2,4).



and  $u_{1s}$ .

Solid curve in the figure indicate the following experimental equation obtained by Nikuradse;

$$\ell/R = 0.14 - 0.08(r/R)^2 - 0.06(r/R)^4 \quad (18)$$

In this equation, the minimum distance  $z$  is replaced by the radial distance  $r$ , since this equation is obtained for the fully developed velocity profile in a straight pipe.

Although the experimental data are considerably dispersive, if we consider that the dispersion of turbulence shear stress  $\tau_{12}$  indicated in Fig.4 is little enough, the origin of this dispersion seems to be mainly attributable to the estimation inaccuracies of the radial gradient of the time-mean velocity  $\bar{u}_1$ . This dispersion is considerable at the region near zero velocity gradient located in the secondary field. The secondary reason of dispersion spreading over the whole regions is supposed to depend on the non-homogeneity of the turbulence exchange and generation. Excluding the non-homogeneity, as is usually practiced when the mixing length model being applied, the following conclusion can be drawn; it is seemed that the relationship between the mixing length and the minimum distance to the wall in the complex flow field near the nozzle port is identical to those for the fully developed velocity profile in the straight pipe.

Figure 7 shows the changes of the coefficients of self correlation  $R_1$  and  $R_2$  to the time interval of  $\tau$ . These figures are illustrated for four places of  $r = 0$  mm, 2 mm, 6 mm and 14 mm. The differences in the value of  $R_1$  and  $R_2$  ranging from  $\tau = 0$  sec to 0.01 sec for first two positions of  $r = 0$  mm and 2 mm indicate the aforementioned non-homogeneity of turbulence. On the contrary to this state, the small differences of  $R_1$  and  $R_2$  for the last two positions show that the conditions of homogeneity are spreading over the secondary flow field.

The Lagrangian scales of turbulence  $\ell_{1,L}$  or  $\ell_{2,L}$  are equal to the product of  $\sqrt{\bar{u}_1 \bar{u}_2}$  and the area bounded by the coordinates and the curves of  $R_1$  or  $R_2$ . The  $\ell_{1,L}$  and  $\ell_{2,L}$  may be considered as the scales for axial and radial directions respectively.

In Fig.8 these scales are plotted as a function of radial position. Although each scales take large values in the vicinity of center line and the outside wall, they become small in the middle region. It will be noticed that the experimental data for the mixing length ( Fig. 5.) and for the Lagrangian length scale ( Fig. 8. ) exhibit quite different behaviour, those for  $\ell$  displaying comparatively smaller values in the secondary flow field than those for  $\ell_{1,L}$  or  $\ell_{2,L}$ .

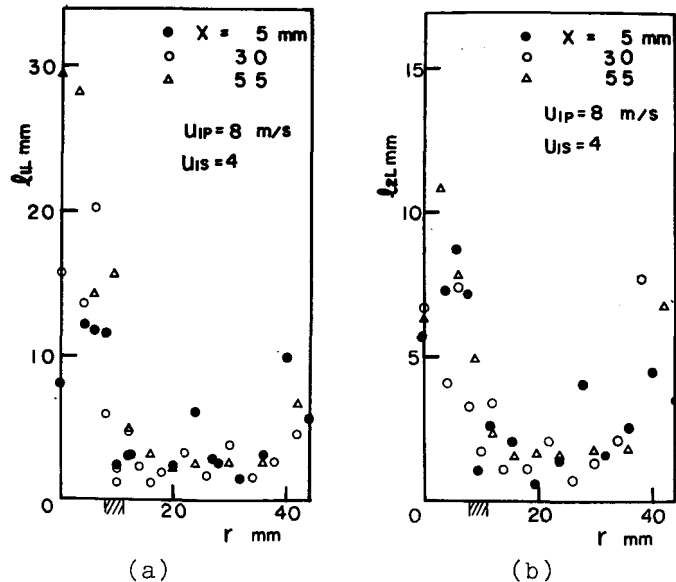


Fig.8. Lagrangian lengths  $\ell_{1,L}$  and  $\ell_{2,L}$  as a function of radial distance  $r$ .

## 6. Concluding remarks.

Based on the results presented here, the following conclusions can be drawn for conditions studied ;

(1) Two dimensional arrangement was done for the time-mean velocity profiles. By this arrangement it become possible to estimate easily two dimensional changes of mixing length.

(2) The measured results of mixing length reinforce the assumption that the mixing length may be expressed as a function of the minimum distance to the nearby solid wall.

(3) Studies were made on the propriety of using the Lagrangian scales of turbulence instead of the mixing length. However, on the contrary to our expectation it is found out from the comparison of measured distributions that the mixing length can not be reasonably estimated from Lagrangian length scales.

## References.

- (1) Y. Tanaka and Y. Shimamoto , Preprint of Japanese 11-th Symposium on Combustion , 11(1973), 213.
- (2) Y. Tanaka and Y. Shimamoto , Preprint of Japanese 12-th Symposium on Combustion , 12(1974), 89.
- (3) J. Nikuradse , VDI Forschungsheft , 356(1932) , also appeared in the book ; S. Kitsuka, A. Hirata and A. Murakami, Heat and Mass Transfer for Chemical Engineers , (1973), 151 .
- (4) I. Tani and Y. Kobashi , Proc. 1st Japan Nat. Congr. Appl. Mech., (1951), 223 .